Arabian Journal of Chemistry 16 (2023) 105264

Contents lists available at ScienceDirect

Arabian Journal of Chemistry

journal homepage: www.sciencedirect.com

Original article

Chemically reactive and thin film flow analysis of cross nano-liquid over a moving surface

Latif Ahmad [a,*], Muhammad Latif [a], Sayed M. Eldin [b]

[a] Department of Mathematics, Shaheed Benazir Bhutto University, Sheringal, Dir Upper 18000, Pakistan
[b] Center of Research, Faculty of Engineering, Future University in Egypt, New Cairo 11835, Egypt

ARTICLE INFO

Article history:
Received 12 February 2023
Accepted 10 September 2023
Available online 12 September 2023

Keywords:
Cross liquid
Buongiorno nanofluid model
Thin film flow
Binary chemical reaction
Film thickness
Numerical solution

ABSTRACT

Vapour generalized liquids hydrodynamics plays a pivotal role in the absorption columns or design of distillation using structured packing since they indomitable the fluid dynamics restrictions of the columns and control rates of mass balance which is the main purpose of this particular work. Particularly, a first attempt is made regarding this work to explore an investigation for time-dependent thin film flow of Cross nano-liquid over a moving surface. Additionally, some physical aspects during this illustration in terms of heat absorption/generation, thermal radiation, magnetic field, non-constant thermal conductivity, and activation energy with chemical reaction are studied. Some of the suitable similarity variables are introduced to convert the leading problem in the form of ordinary differential equations and then the transformed problem is approximated by one of the built-in collocation methods by using MATLAB. Very interesting results in terms of monotonic reduction in the film thickness for various uplifting values of unsteadiness and magnetic parameters and vice versa for the Wessenberg number are found. Moreover, temperature and concentration are concluded as enhancement functions of variable thermal conductivity and activation energy, respectively. The last comparative work is presented to validate the entire approach and where the method shows an excellent correlation with the previously published results.

1. Introduction

Fluid flow phenomenon is not ignorable due to its numerous uses in daily practices. Its significance attracts many users to the scientific exploration of the liquid flow phenomenon. We can apply these fluids in many disciplines like industries, metallurgical, engineering, mining, chemicals, and civil engineering. Fluids are further classified as Newtonian and non-Newtonian. In these disciplines, many researchers (Sakiadis, 1961; Crane, 1970) reported the importance of Newtonian fluid flow over moving surfaces. Currently, generalized Newtonian fluids (GNF's) have gained huge significance amongst researchers on account of their remarkable practicality, chemical, technological appliances, and industrial sectors. The GNF's (Bird et al., 1976; 1987) explored the viscosity as shear dependent as a result of which a new constitutive relation is defined by making reforms in Newton's law of viscosity to the description for the viscosity change with changing shear rate. The most common type of the GNF's is the power-law fluid (Hassanien et al., 1998), which proposes the simplest representation of the shear-thickening/thinning behaviors of numerous liquids. (Horrigue and Abbas, 2020) provided an explanation of the Fractional-Order Thermo-elastic wave assessment in a two-dimensional Fiber-Reinforced Anisotropic material. In a two-dimensional media with voids, (Hobiny and Abbas, 2020) investigated the assessment of fractional-order thermo-elastic waves. (Wang et al., 2022) numerical analysis of the melting and entropy generation of the infinite shear rate Carreau model over the Riga plate with unpredictable thickness. The tilted magnetized and energy transmission aspects of the Carreau nano-fluid with infinite shear rate viscosity model were explored by (Shah et al., 2022). (Ayub et al., 2022) investigated the magnetized Carreau nanofluid's infinite shear rate viscosity and heat transfer.

However, the massive application of non-Newtonian fluids in engineering and industry attracts many researchers to analyze the significance of such materials. Particularly, the uses of non-

* Corresponding author.
E-mail address: latifahmad@sbbu.edu.pk (L. Ahmad).

Peer review under responsibility of King Saud University.

Production and hosting by Elsevier

https://doi.org/10.1016/j.arabjc.2023.105264
1878-5352/

Nomenclature

Γ,n	material constants
(x,y)	Cartesian coordinates
U_s	surface velocity
V	velocity vector
(u,v)	components of velocity
ρ	fluid density
η	variable with no dimension
F	dimensionless stream function
(qw,jw)	heat and mass fluxes at the wall
ν_f	kinematic liquid viscosity
t	time
p	the pressure
k(T)	thermal conductivity
T	temperature of the fluid
(T_0,T_s)	The slite reference temperatures
α	stretching parameter
σ	stepan Boltzman constant
β	film thickness
C	nanoparticle volume friction
h(t)	hight of thickness
(C_0,C_s)	The slite reference concentrations
U_e	stagnation velocity
D_B	Brownian diffusion coefficient
D_T	thermophoresis diffusion coefficient
ψ	stream function
θ	dimensionless temperature
φ	dimensionless concentration
τ_w	shear stress at wall
δ	chemical reaction parameter
C_p	specific heat
B_0	applied magnetic field
C_f	skin friction related coefficient
α	liquid thermal diffusivity
μ	liquid dynamic viscosity
K	chemical reaction constant
A	time parameter
N_{ux}	local Nusselt number
Sh_x	local Sherwood number
W_e	Wessenberg number
c	time constant
τ	ratio parameter
λ_1	heat generation/absorption
H_a	magnetic parameter
E_a	Activation energy parameter
Pr	Prandtl number
Sc	Schmidt number
N_b	Brownian motion parameter
N_a	thermophoresis parameter

Newtonian fluids in our daily life are in the form of honey, paints, blood, and toothpaste. Many mathematical models have been created to predict some aspects of such fluids in nature. Initially, (Acrivos et al.,1960) and (Schowater, 1960) examined heat transfer on a horizontal flat plate At the boundary layer, non-Newtonian fluids flow as rapidly as possible. Cross fluid (Cross, 1965) is one of the prominent subclasses of GNFs. In fact, this fluid is non-Newtonian in nature. In order to characterize the surface layer conduct of Cross fluid, the axisymmetric flow of Cross fluid above a radially on the move surface was initially observed by (Khan et al., 2017). (Hayat et al., 2017) discussed the velocity and temperature distributions during the Cross-fluid flow. Recently, the Power-law fluids in the presence of Lorentz forces have been studied by several authors (Ayub et al., 2022; Shah et al., 2022; Rehman et al., 2023).

(Choi, 1995) was the pioneer to introduce the term nano-fluid. This new phenomenon has many advantages in the field of nanotechnology, but one of the most advantages in terms of enhancement in the thermal conductivity of liquids is playing a vital role in fluid flows. In this regard, (Buongiorno, 2006) discovered that when nanoparticles are added, seven slip mechanisms emerge, as a result, the nanoparticles and the base fluid move at the same speed. He came to the conclusion in nano-fluid flow, where the primary slide effects are thermophoresis and Brownian diffusion. (Khan and Pop, 2010) used computer techniques to study laminar nano-fluid flow across a linearly stretched sheet and found comparable results. In order to account for the impacts of internal heating, (Lin et al., 2015) investigated the flow and heat transmission of MHD pseudo-plastic nano-fluid in a finite film over an unstable stretching surface. (Khan et al., 2017) used nanoparticles to investigate chemical processes that have an impact on the generalized Burgers fluid. Some scientists have reported the composite of tin cobalt oxide nanoparticles with graphene oxide for the application of RB5 dye degradation and the application as a fuel additive (Jamil et al,. 2017; 2018; Khan et al,. 2018; Jamil et al,. 2018; 2021; Naz et al,. 2022). Unsteady Walter's B nano-fluid flow on a vertical cylindrical disk was studied by (Ahmad et al., 2022). Then, the nanoscale energy transfer of inclined magnetized 3D hybrid nano-fluid with the Lobatto IIIA scheme was explored by (Ayub et al., 2021). Another very remarkable illustration of the flow of liquid with the addition of heat and mass balance was explored by (Shao et al., 2022). Studied the Homann flow of visco-elastic materials with the impact of novel microorganism as well as nanoparticles during heat and mass transportation. The natural convective flow of a magnetic hybrid nano-fluid in an altered porous trapezoidal enclosure was statistically analyzed by (Chabani et al., 2022). The motion of Oldroyd-B nano-liquid with hydromagnetic bio-convection via a porous stretched surface was studied by (Ould Sidi et al., 2023). Many researchers, like (Ullah et al., 2023; Wang et al., 2023; Jamil et al., 2023) are completed this type of attempt to express its practicality.

The word Arrhenius energy was first time coined by Svante Arrhenius. Activation energy is the amount of energy to initiate a chemical reaction. This type of energy does not remain the same for different chemical reactions even if it becomes sometimes zero for particular reactions. The quantity of activation energy varies for different chemical processes, even though sometimes it is zero. Binary chemical reaction parallel with this kind of energy exists in the heat and mass balance phenomenon and have practical applications in the field of geothermal reservoir, chemical engineering, food processing, and emulsion of various suspensions, etc. In this regard, (Bestman, 1990) pioneered this type of chemical reaction. In the presence of a chemical reaction and non-Darcian and non-rigid, (Mohamed et al., 2009) examined the significance of hydro-magnetic motion with the parallel movement of heat and mass balance. In fractional order thermo-elastic media, the plane deformation caused by heat source was explored by (Kumar et al., 2013). (Lazaridis et al., 2014), where they reported that a successful reaction with a certain non-zero probability will be assumed reasonably. (Shafique et al., 2016) addressed that activation energy has the key component during the binary chemical reaction. Another pioneering researcher (Hsiao, 2017) reported

the same chemical reaction throughout the flow of viscous liquid in the presence of the applied magnetic field. The use of this particular phenomenon contains the capability to promote economic efficiency. (Mustafa et al., 2017) elucidated the magneto-hydrodynamics flow over moving surfaces in the presence of Activation energy and Binary chemical reaction. Where they explored zero mass flux conditions, while the heating transmission is noticed in reduction conduct by improving the chemical reaction. (Manzur et al., 2020) conducted a computational analysis of the Falkner Skan flow of a chemically reactive Cross-nanofluid with heat production or absorption. (Khan et al., 2018) approximated the Casson nano-liquid flow by incorporating Activation energy parallel with Binary chemical reaction in the presence of an irreversible process. Where the authors found that such energy is required to perform the said chemical reaction. The most recent investigation of Activation energy and chemical reaction is studies by (Anjum et al., 2022) and (Bilal et al., 2022). Thermodynamic analysis for bio-convection peristaltic transport of nanofluid with gyrotactic motile microorganisms and Arrhenius activation energy was performed by (Akbar et al., 2022).

The analysis of flow characteristics by considering the thin-film phenomenon has had significant importance in different areas of engineering and technology during the last few decades. However, many well-known applications in the form of polymer and metal extrusion, constant forming, fluidization of the devices, etc, are noticed by considering the thin-film phenomenon. In this regard, (Wang, 1990) was the first who reported that time depended on the thin-film flow of liquid. (Anderson et al., 1996) elaborated on the effect of thin-film fluid on non-linear stretching surfaces. (Aziz and Hashim, 2010) reported the impact of viscous dissipation with general surface conditions during the thin film liquid flow. (Aziz et al., 2011) explored the significance of internal heating, while describing the thin-film flow over a moving surface. (Bachok et al., 2012) and (Xu et al., 2013) addressed the finite thin-film concept with heat balance during the moment of the surface of configuration. Theoretical examination of thermal damage to skin tissue brought on by powerful moving heat source (Hobiny and Abbas, 2018). The fractional transient heating that occurs inside the skin tissue during thermal treatment was the subject of an analytical investigation by (Ghanmi and Abbas, 2019). The effects of magneto-hydrodynamic flow through a vertical plate with varying surface temperatures were investigated by (Abbas et al., 2010). The free convection MHD flow with heat radiation from an abruptly starting vertical plate was studied by (Palani and Abbas, 2009). (Lin et al., 2014) discussed the MHD thin-film and heat transfer of power-law fluids over an unsteady stretching sheet with variable thermal conductivity. Using a second-grade fluid with variable thermal conductivity, (Haider et al., 2021) investigated energy transference in time-dependent Cattaneo-Christov double diffusion. (Li et al., 2016) examined the heat generation and thermo-phoresis characteristics of an unstable magneto-hydrodynamics (MHD) thin-film fluid flow over a finite thin sheet and nano-fluid radiation heat transfer.

To overcome, the unexplored physical phenomenon, Cross fluid thin film flow is carried out in this particular work. Additionally, thin film Cross liquid flow is analyzed with combined effects of the magnetic field, heat generation, thermal radiation, variable thermal conductivity, and Activation energy. Both mass and heat balance aspects are deliberated in the presence of Brownian motion and thermophoresis phenomena. The key outcomes are illustrated by implementing one of the collocation methods in MATLAB.

The entire work is organized as follows:

Section 2 presents the problem formulation with some assumptions and the transfer of mass and heat with the flow is also part of the subsections. In Section 3, similarity-related variables are defined for the conversion of PDEs to ODEs. Sections 4 and 5 present the whole analysis in the form of ODEs. Section 6 presents the practical quantities related to the whole analysis. Section 7, is about to present the numerical scheme as employed for finding the numerical solution. Section 8 presents the results and discussion of the entire work. In section 9, a comparison with previous work is presented. In the last section 10, a brief conclusion is provided with some novel findings.

2. Problem formulation

Let us assume that the flow of Cross nano-fluid over an electrically condensing moving surface. Here, in this study, the surface is configured with a thin film concept as shown in Fig. 1, with film thickness h(t). Where a narrow slit starts from the origin in terms of Cartesian coordinates. The surface is moved with the influence of the transient velocity, $u = U_s = \frac{ax}{1-ct}$ at $v = 0$, where a and c are constants. The slit reference temperature is considered in the form of T_0, C_0, and T_s, C_s, respectively. By taking into concentration the magnitude field normal to the surface, while the neglected the induced magnitude field due to the following low Reynolds number theory.

2.1. Flow analysis

In order to investigate about the motion of the liquid model introduced by (Aziz et al., 2011; Manzur et al., 2020) is further explored by plugging the following velocity vector;

$$\vec{V} = [u(x, y, t), \quad v(x, y, t), \quad 0]. \tag{1}$$

The newly formulated problem is then displayed below:

$$\frac{\partial u}{\partial t} + u.\left(\frac{\partial u}{\partial x}\right) + v.\left(\frac{\partial u}{\partial y}\right) = -\left(\frac{1}{\rho}.\frac{\partial p}{\partial x}\right) + \nu_f.\frac{\partial}{\partial y}\left[\frac{\frac{\partial u}{\partial y}}{1 + [\Gamma.\left(\frac{\partial u}{\partial y}\right)]^n}\right] + \frac{\sigma}{\rho_f}.B_0^2.(U_s - u). \tag{2}$$

Subjected the BC's

$$u = U_s = \frac{a.x}{1 - c.t}, \quad v = 0, \quad at\ y = 0, \quad \frac{\partial u}{\partial y} = 0, \quad v = \frac{dh}{dt}\ at\ y = h. \tag{3}$$

2.2. Heat and mass transfer analysis

In order to explore the significance of nano-fluid, variable thermal conductivity, thermal radiation, heat generation/absorption, and activation energy during the thin film flow of Cross fluid, we need to use the temperature and concentration fields in the following way.

$$[T = T(x, y, t), C = C(x, y, t)]. \tag{4}$$

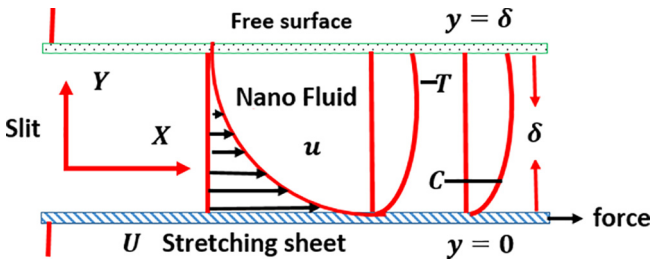

Fig. 1. Thin film flow configuration.

Substitution of the above equation, we arrived to formulate the energy and concentration equations in the following way and as expressed by (Aziz et at, 2011).

$$\left[\begin{array}{c}\frac{\partial T}{\partial t}+u.\left(\frac{\partial T}{\partial x}\right)+v.\left(\frac{\partial T}{\partial y}\right)=\frac{1}{(\rho c)_f}.\frac{\partial}{\partial y}\left(k(T)\frac{\partial T}{\partial y}\right)+D_B.\tau.\left(\frac{\partial C}{\partial y}.\frac{\partial T}{\partial y}\right)+\\ \left(\frac{D_T}{T_\infty}\right).\tau.\left(\frac{\partial T}{\partial y}\right)^2+\frac{Q.(T-T_\infty)}{(\rho c)_f}-\frac{1}{(\rho c)_f}.\left(\frac{\partial q_r}{\partial y}\right)\end{array}\right], \tag{5}$$

$$\left[\begin{array}{c}\frac{\partial C}{\partial t}+u.\left(\frac{\partial C}{\partial x}\right)+v.\left(\frac{\partial C}{\partial y}\right)=D_B.\left(\frac{\partial^2 C}{\partial y^2}\right)+\frac{D_T}{T_\infty}.\left(\frac{\partial^2 T}{\partial y^2}\right)+\\ {K_c}^2.(C-C_0).\left(\frac{T}{T_0}\right)^n.exp\left(-\frac{E_a}{k(T).T}\right)\end{array}\right], \tag{6}$$

where $\tau=\frac{(\rho c_p)_n}{(\rho c_p)_f}$ is the ratio of heat capacity of nanoliquid and base liquid, $k(T)$ and q_r are the variable thermal conductivity and thermal radiation coefficient, respectively, are expressed as:

$$k(T)=k_s.\left(1+\in.\frac{T-T_0}{T_s-T_0}\right), \tag{7}$$

$$q_r=-\frac{4.\sigma^*}{3.k^*}\frac{\partial T^4}{\partial z}=-\left(\frac{16.\sigma^*}{3.k^*}\right).\frac{\partial}{\partial y}\left(T^3.\frac{\partial T}{\partial y}\right). \tag{8}$$

Associated BC's are stated as:

$$T=T_s, C=C_s, at\ \ y=0, \frac{\partial T}{\partial y}=\frac{\partial C}{\partial y}=0,\ \ as\ \ \ y=h. \tag{9}$$

3. Similarity analysis

To find the solution of Eqs.(2), (5), (6) with BC's (3) and (9), we need to first transform these into ODEs and then apply one of the collocation techniques while using MATLAB. In this regard, the following local similarity variable is defined as:

$$u=U_s f'(\eta),\quad v=-\sqrt{\frac{v.x}{1-c.t}}f(\eta),\quad \theta(\eta)=\frac{T-T_0}{T_s-T_0},\quad \phi(\eta)=\frac{C-C_0}{C_s-C_0},\quad \eta=y.\sqrt{\frac{U_s}{v_f x}}, \tag{10}$$

where

$$T_s=T_0+\frac{T_0.U_s.x}{v.(1-c.t)^{\frac{1}{2}}},\quad C_s=C_0+\frac{C_0.U_s.x}{v.(1-c.t)^{\frac{1}{2}}}, \tag{11}$$

with film thickness

$$\beta(t)=\frac{\beta_0}{(1-c.t)^{\frac{1}{2}}}. \tag{12}$$

4. Flow analysis ODE's

Thin film Cross fluid flow governing Eqs.(2) and (3), as the PDEs are highly non-linear and which need to transform into ODEs. Thus these PDEs are transformed into ODEs by using the local similar variables defined through Eqs.(10)-(12), we get.

$$\left[1+(1-n)\left(We.f''\right)^n\right].f'''+\left[f.f''-f'^2\right].\left[1+\left(We.f''\right)^n\right]^2 -\left[A.\left(f'+\frac{\eta}{2}.f''\right)\right].\left[1+\left(We.f''\right)^n\right]^2-H_a^2.(f').\left[1+\left(We.f''\right)^n\right]^2=0, \tag{13}$$

with BC's are

$$f(0)=0,\ f'(0)=1,\quad f(\beta)=\frac{A.\beta}{2},\ f''(\beta)=0. \tag{14}$$

4.1. Dimensionless parameters

The physical dimensionless quantity are listed as:

S. No	Parameter	Mathematical form
1	Unsteadiness parameter (A)	$\frac{c}{a}$
2	Hartmann number (H_a^2)	$\frac{\sigma {B_0}^2}{\rho_f a}$
3	Wessenberg number(We)	$c\Gamma Re^{\frac{1}{2}}$
4	Reynolds number(Re)	$\frac{x.U_s}{v_f}$

5. Heat and mass transfer analysis ODE's

In a similar way, the PDEs of energy and concentration Eqs.(5) and (6) along with BCs defined in Eq.(9), are transferred into ODEs by using local similar variables defined through Eqs.(10)-(12). Thus resulting local non-similar ODEs are given as;

$$\frac{d}{d\eta}\left[\left\{1+R_d.\left\{1+\left(\theta_f-1\right).\theta\right\}^3\right\}.\theta'\right]+Pr.\left(f.\theta'-2.f'.\theta\right)-Pr.\left(\frac{A}{2}\right).\left(\eta.\theta'+3.\theta\right) +Pr.N_b.\theta'.\varphi'+Pr.N_t.\theta'^2+\lambda_1.Pr.\theta+(\in.).\theta''+\in\theta'^2, \tag{15}$$

$$\varphi''+Pr.Le.\left(f.\varphi'-2.f'.\varphi'\right)-\mathrm{Pr}.Le.\frac{A}{2}.\left(\eta.\varphi'+3.\varphi\right)+ \left(\frac{N_t}{N_b}\right).\theta''-Pr.Le.\sigma.\varphi(1+\delta.\theta)^n.\exp\left(-\frac{E_1}{1-\delta.\theta}\right)=0, \tag{16}$$

$$\theta(0)=1,\quad \varphi(0)=1,\ \ \theta'(\beta)=0,\ \ \varphi'(\beta)=0. \tag{17}$$

5.1. Dimensionless parameters

The non-dimensional quantities are listed as:

S. No	Parameter	Mathematical form
	Radiation parameter (R_d)	$\frac{16\sigma^* {T_s}^3}{3k^* k_s}$
	Thermal ratio parameter (θ_f)	$\frac{T_f}{T_s}$
	Electrical conductivity(σ)	$\frac{{K_c}^2}{a}$
	Chemical reaction energy parameter(δ)	$\frac{(T_f-T_s)}{T_s}$
	Activation energy (E_1)	$\frac{E_a}{kT_s}$
1. ‘	Prandtl number(Pr)	$\frac{v_f}{\alpha}$
	Thermal diffusivity (α)	$\frac{k_s}{(\rho c_p)_f}$
	Brownian motion (Nb)	$\frac{C_s D_B \tau}{v_f}$
	Thermophoresis parameter (Nt)	$\frac{D_T \tau}{v_f}$

6. Engineering quantities

In order to scrutinize the impact of resistive forces, rate of heat, and mass balance during the thin film flow of Cross liquid, we need to approximate the subsequent quantities as:

(a) Skin friction

For the skin fraction, the coefficient C_f is defined as,

$$C_f = \frac{2.\tau_w}{\rho_f.U_s^2}, \tag{18}$$

where

$$\tau_w = \left[\eta_0.\frac{\frac{\partial u}{\partial y}}{1+\{\Gamma.\left(\frac{\partial u}{\partial y}\right)\}^n}\right]_{y=0}, \tag{19}$$

By putting Eqs.(10)-(12) and (19) in Eqs.(18), we have

$$\frac{1}{2}.\mathrm{Re}^{\frac{1}{2}}.C_f = \frac{f''(0)}{1+\left(We.f''(0)\right)^n}, \tag{20}$$

where $\mathrm{Re} = \frac{x.U_s}{\nu_f}$.

(b) Local Nusselt number

To approximate rate of heat, transfer, we need to define the local Nusselt number as below:

$$Nu_x = \frac{x.q_r}{k.(T_s - T_0)}|_{y=0}\left[-\frac{x}{T_f - T_0}.\frac{\partial T}{\partial y}\right]_{y=0}. \tag{21}$$

By plugging Eqs.(10)-(12) in to Eq.(21), we have

$$\mathrm{Re}^{-\frac{1}{2}}.Nu_x = -\left[1+R_d.\left(1+\left(\theta_f-1\right).\theta\right)^3.\theta'(0)\right] + \frac{x.q_w}{k.(T_f - T_0)}. \tag{22}$$

(c) Local Sherwood number

To determine the mass transfer rate during the thin film Cross liquid flow, we need to defined Sherwood number as below:

$$Sh_x = \left[-\frac{x}{C_f - C_0}.\frac{\partial C}{\partial y}\right]_{y=0}. \tag{23}$$

Then by utilizing Eqs. (10)-(12) into Eq.(23), we have

$$\mathrm{Re}^{-\frac{1}{2}}.Sh_x = -\varphi'(0). \tag{24}$$

7. Applied numerical scheme

In this section, the numerical approach is explained along with its procedures for the present problem considered in terms of the thin film flow of Cross nano-liquid. However, more physical deterministic effects are being assumed in the presence of non-variable thermal conductivity, magnetic field, AE with BCR and heat generation are embedded in the leading equations. The resulting equations create complexities during its exact solution and required more time for analytical findings. The numerical scheme implementation requires the problem as a system of first order ODEs, together with surface and for away constraints. The built-in collocation formula in MATLAB can be applied with default fourth order accuracy in the specified interval. However, the proposed numerical scheme is basically using the finite difference approach for the modification of initial guess and the entire method based on the three-stage Lobatto relation. The basics procedures are listed as below:

$$\chi_1 = f,\ \chi_2 = f',\ \chi_3 = f'',\ \chi\chi_1 = f''', \tag{25}$$

$$\chi_4 = \theta,\ \chi_5 = \theta',\ \chi\chi_2 = \theta'', \tag{26}$$

$$\chi_6 = \varphi,\ \chi_7 = \varphi',\ \chi\chi_3 = \varphi'', \tag{27}$$

$$\chi\chi_1 = \frac{-\left(\chi_1\chi_2 - \chi_2^2\right)\left(1+\left(We\chi_3\right)^n\right)^2}{\left(1+(1-n)\left(We\chi_2\right)^n\right)} + \frac{A\left(\chi_2 + \frac{\eta}{2}\chi_3\right)\left(1+\left(We\chi_3\right)^n\right)^2}{\left(1+(1-n)\left(We\chi_2\right)^n\right)} + \frac{H_a^2\chi_2\left(1+\left(We\chi_3\right)^n\right)^2}{\left(1+(1-n)\left(We\chi_2\right)^n\right)}, \tag{28}$$

$$\frac{d}{d\eta}\left(\{1+R_d\{1+\left(\theta_f-1\right)\chi_4^3\}\chi_5\right) + Pr\left(\chi_1\chi_5 - 2\chi_2\chi_4\right) - \mathrm{Pr}\left(\frac{A}{2}\right)\left(\eta\chi_1 5 + 3\chi_4\right) + PrN_b\chi_5\chi_7 + \mathrm{Pr}N_t\chi_5^2 + \lambda_1\mathrm{Pr}\chi_4 + \left(\in\chi_5\right)\chi\chi_2 + \in\chi_5^2 = 0, \tag{29}$$

$$\chi\chi_3 = -PrLe\left(\chi_1\chi_7 - 2\chi_2\chi_6\right) + \mathrm{Pr}Le\frac{A}{2}\left(\eta\chi_7 + 3\chi_6\right) - \frac{N_t}{N_b}\chi\chi_2 + PrLe\sigma\chi_6(1+\delta\chi_4)^n\exp\left(-\frac{E_1}{1-\delta\chi_4}\right). \tag{30}$$

With BC's are

$$\chi_1(0) = 0,\ \ \chi_2(0) = 1,\ \ \chi_1(\beta) = \tfrac{A\beta}{2},\ \chi_3(\beta) = 0,\quad \chi_4(0) = 1,\ \ \chi_6(0) = 1,\ \ \chi_5(\beta) = 0,\ \ \chi_7(\beta) = 0. \tag{31}$$

8. Results and discussion

This section includes a discussion of the new results approximated during the modification in terms of the thin film aspect, while considering the flow equations developed by (Manzoor et al., 2020). The leading parameters regarding the thin film flow over a moving boundary produces significant impacts on Cross liquid velocity, temperature, and concentration. Furthermore, effective new parameters during this particular flow are also tested, while approximating the behavior of thin film thickness β. Many other parameters, like the Wessenberg number (We), Hartman number (Ha), variable thermal conductivity $(\in)$, thermal radiation parameter (Rd), heat generation/absorption parameter (λ_1), electrical conductivity (σ) and activation energy parameter E_1 are interpreted during the plots and other outputs. Particularly, the liquid velocity, temperature, and concentration results analysis are performed to enhance the quality of the entire work.

To elaborate on the importance of each leading flow parameter, we need to fix the other parameters in the form of $We = 0.2, A = 1.5$ and $Ha = 0.2$, on the other hand, to describe the thermal and concentration features for fixed parameters, $We = 3.0, A = 1.5, Nb = 0.2, Ha = 0.2, Nt = 0.5, Pr = 1.2, \lambda_1 = 0.5, \epsilon = 1.0, \theta_f = 1.1, E_1 = 1.0, Rd = 2.0, Le = 2.0, \delta = 0.2, \sigma = 0.4$ and $m = 0.2$.

Through Fig. 2, a variation in We, i.e., varying from 0.2 to 0.8 which produces escalation in the liquid velocity with parallel monotonic uplifting variation in β. A very authentic reason is provided to explain this escalation in velocity in terms of enhancement in the thermal relaxation time leads to improve the Cross liquid velocity. The MBLT is reduced during this variation. A significant uplifting influence in the liquid velocity during the variation in A is noted with parallel monotonic reductive variation in film thickness as shown in the same Fig. 2. From practical point of view, with such higher values in the said parameter making the buoyance forces stronger as compared to the lower time parameter. On the other hand, the film thickness is found with weaker demea-

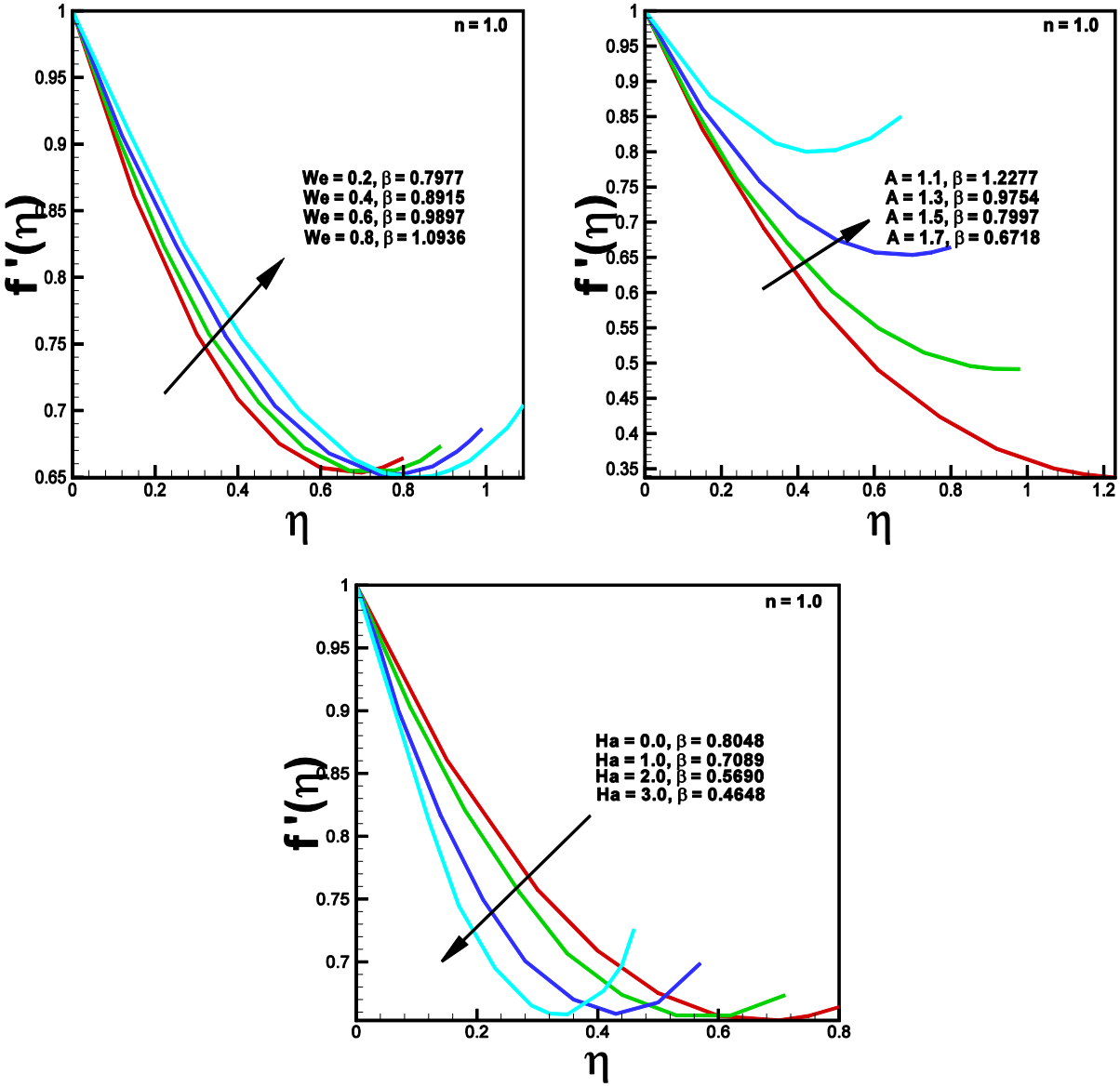

Fig. 2. Impact of Wessemberg (We), unsteadiness (A) and Hartman (Ha) on velocity field $f\prime(\eta)$, respectively.

nor. The liquid velocity is decreasing function of *Ha* as presented through the aforementioned Fig. 2. In a physical sense, it is much clear that whenever *Ha* is taken in higher order, the Lorentz forces are uplifted and cause a reduction in the velocity. Fig. 3, is presented to show the impact of *Nb* on the temperature of the material, whereas the temperature is escalated during this particular flow. Physically, this is due to an increase in the Brownian motion of the liquid particles which causes enhancement in heat transfer from the lower surface to the upper region. The related TBLT is also reducing during this variation. The same Fig. 3, also demonstrates the impact of *Nt* on the temperature of the liquid with escalation. From a physical point of view, whenever, an escalation in *Nt* is produced, the thermophoretic forces also increased which causes more heat transfer in specific cases of the flow of liquid. The related TBLT is noticed with higher conduct. In Fig. 4, the defect of *Rd was* tested to show the nature of the liquid temperature with increasing demeanor. In a physical sense, it is illustrated that whenever radiation is increased during this particular flow, an escalation is produced in the thermal properties of the liquid. In the same Fig. 4, also illustrates the behavior of *Pr* on the temperature of the liquid with reduction conduct. From a physical point of view, if this quantity *Pr* is increased, the thermal conductivity is reduced and which causes reduction in temperature. The related TBLT increased during this flow. Through Fig. 5, a significant enhancement in the temperature of the liquid particles is noticed during the variation in λ_1. This increase in the heat source parameter physically added more heat to the temperature domain. Through the same Fig. 5 it is sketched to show the behavior of ϵ on liquid temperature with enrichment conduct. This is due to the increase in the variable thermal conductivity in a direct way. Fig. 6 is interpreted to signify the impact of *A* on the temperature of the liquid. It is obvious that when more time is given to the flow duration it leads to reduce the temperature of the liquid. The increasing variation in θ_f on liquid temperature is demonstrated through the preceding said Fig. 6. Physically, these higher values of θ_f enhanced the surface temperature and the liquid temperature remains lower in comparison which causes enhancement in the temperature of the liquid. Fig. 7 is plotted to demonstrate the behavior of liquid concentration with reduction conduct while taking higher values of *Nb*. This is due to the random motion of the liquid molecules

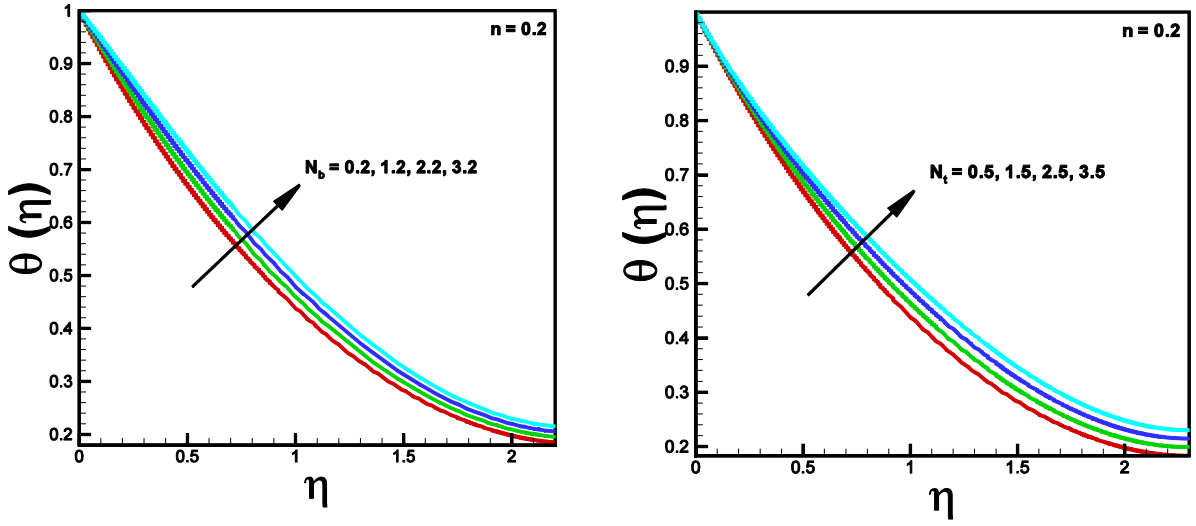

Fig. 3. Impact of Brownian motion (N_b) and thermophoresis (N_t) on temperature $\theta(\eta)$, respectively.

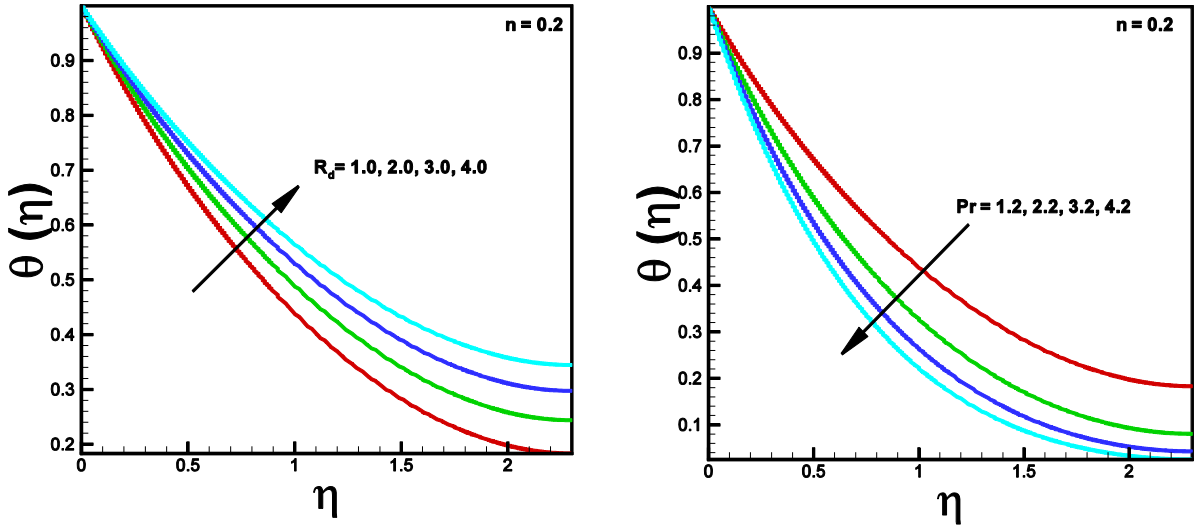

Fig. 4. Impact of radiation (R_d) and Prandtl (Pr) on temperature $\theta(\eta)$, respectively.

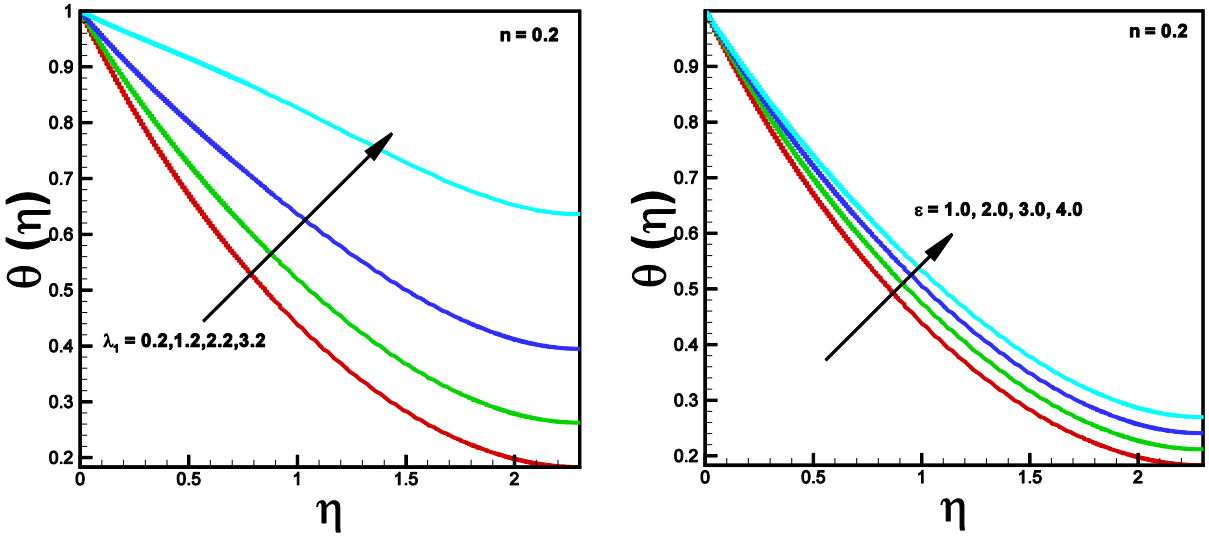

Fig. 5. Impact of heat generation (λ_1) and variable thermal conductivity (ϵ) on temperature $\theta(\eta)$, respectively.

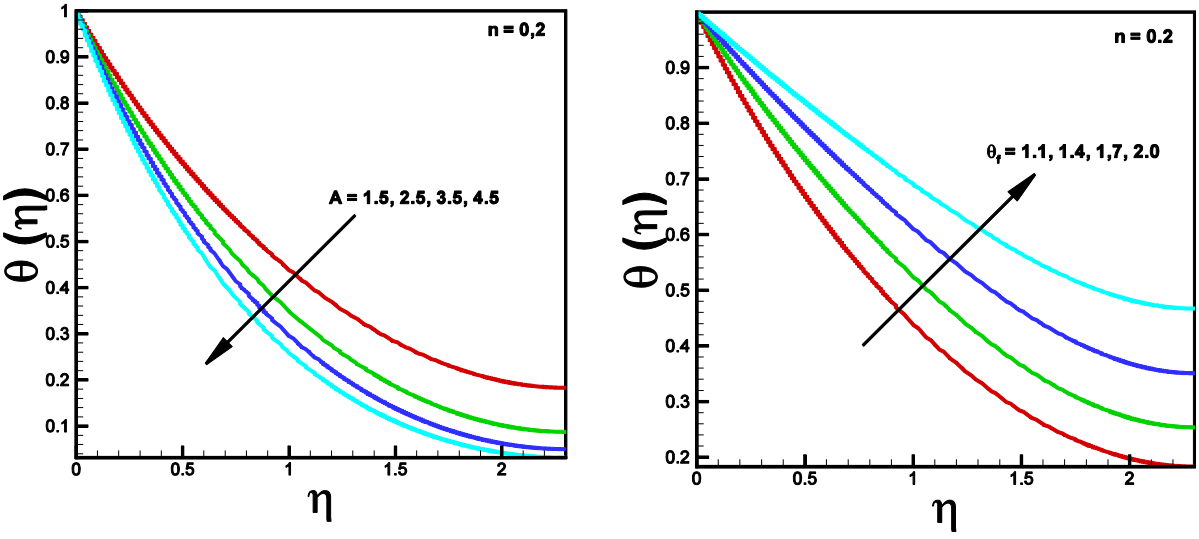

Fig. 6. Impact of unsteadiness (A) and temperature ratio (θ_f) on temperature $\theta(\eta)$, respectively.

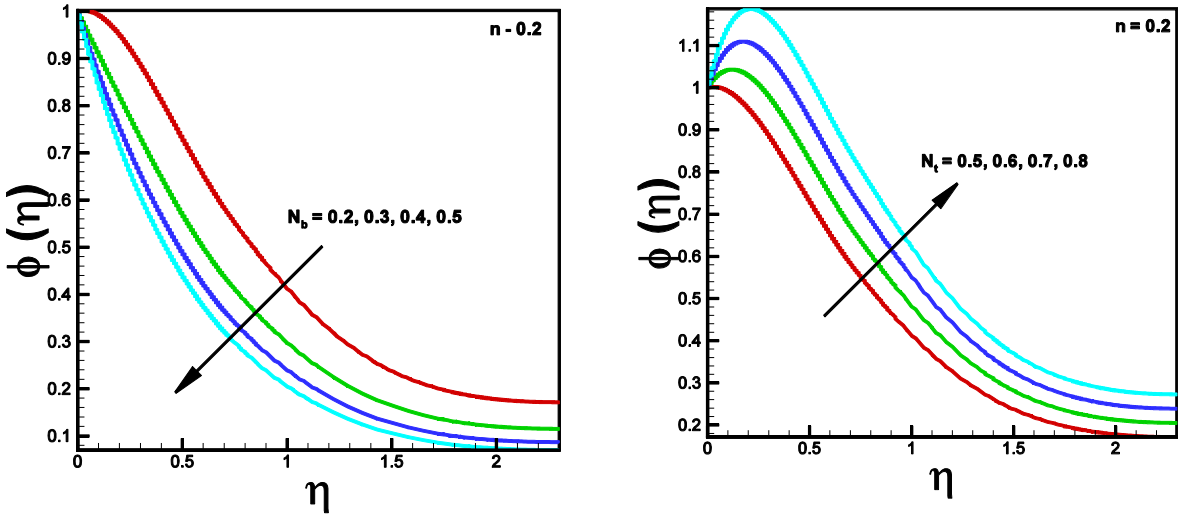

Fig. 7. Impact of Brownian motion (N_b) and thermophoresis (N_t) on concentration $\phi(\eta)$, respectively.

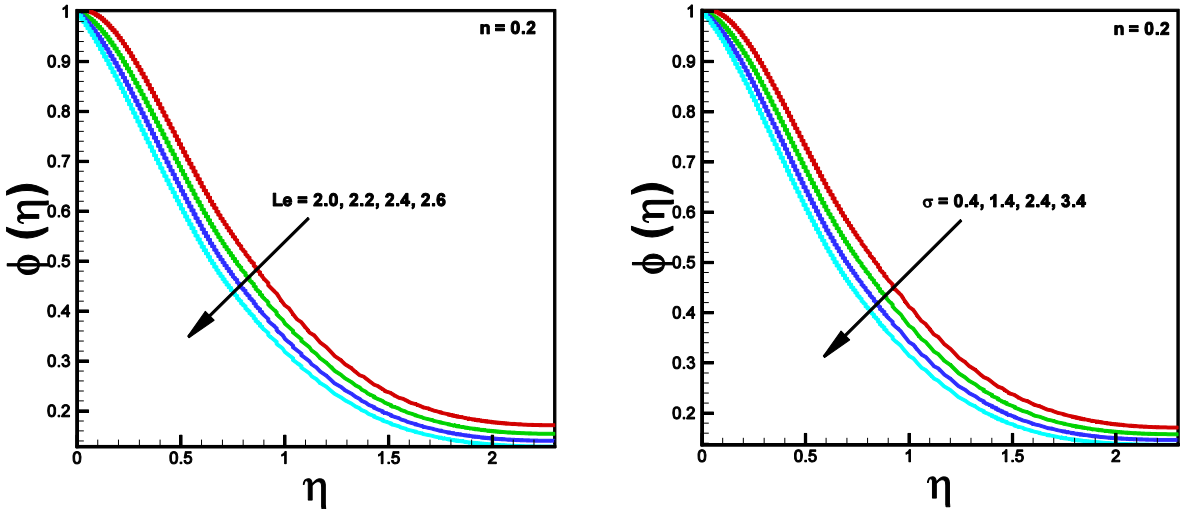

Fig. 8. Impact of Lewis (Le) and electrical conductivity (σ) on concentration $\phi(\eta)$, respectively.

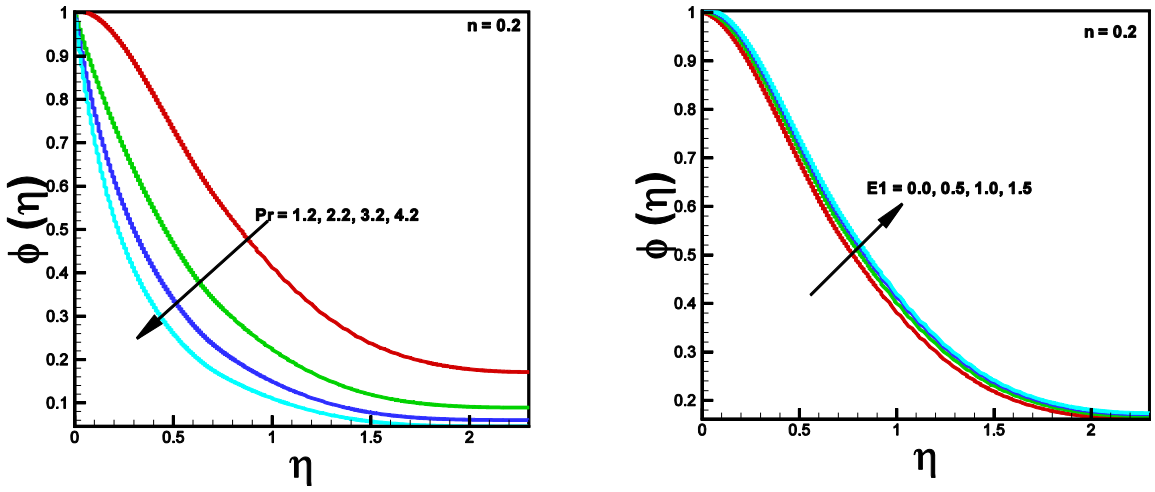

Fig. 9. Impact of Prandtl (Pr) and activation energy (E_1) on concentration $\phi(\eta)$, respectively.

and which is corresponding to the decline in the nanoparticle's concentration. However, by enhancement in this parameter, a reduction is observed inside the viscous dominant region during the motion of the liquid and hence the results are reliable with the predictable one. Additionally, due to enhancement in the indecisive movement of the random in and out molecules of the viscous region and in the free stream is the outcomes of the higher *Nb*. Since the viscous region is relatively smaller than the non-viscous region and which shows that some the nanoliquid molecules enters in the non-viscous region will not may come out to the viscous region. This is why a reduction in the viscous region of the volume fraction is caused. The related CBLT is increased during this variation. In Fig. 7, the uplifting behavior of *Nt* parameter is introduced during the plotting of concentration fields. This physical significant result shows that whenever the thermophoretic forces increase, more mass transferring from the surface has occurred inside the boundary layer motion and where the results are not consistent with the predicable one. Thermo-phoresis clues a movement of the particles toward the cold region from a hotter region. The forming of the gas dissipated projectile is one the application as a result of the removing of small particles from the gas streams. Fig. 8 illustrates a reduction behavior of variation in *Le* on the concentration fields. Physically, the ratio of thermal diffusivity to mass diffusivity defines the Lewis number and which indicates that when this number is taken in increasing order, then mass diffusivity decreased and this is why the concentration of the liquid decreased. Fig. 8 is also configured to show the impact of σ on the concentration of the liquid with declining impact. This is due to an escalation in the electrical conductivity enhancement. Another physical impact of *Pr* on the concentration of the liquid is portrayed in Fig. 9, where a reduction in the concentration is noticed in this particular situation. This reduction in the concentration is due to the reduction in momentum diffusivity. Fig. 9 is also portrayed to introduce increasing conduct of the liquid concentration during the variation in E_1. Physically, the activation type energy is that quantity of energy which is enough to make quickly the chemical process of reaction during the motion of Cross liquid and this is why more transferred of mass is occurred during this particular boundary layer motion. In a practical sense, it is very clear that whenever an enhancement is made in this particular energy parameter, then a weaker temperature is observed. Thus, the result is reliable with the predictable one and the relevant CBLT is also an uplifting function of the aforementioned parameter.

In Table 1, an important reduction impact of film thickness is noticed during the variation in *We*, *Ha* and *A*. The resistive forces

Table 1
Eigenvalue of the film thickness.

A	We	H_a	Film thickness(β)
1	3	0.2	3.5750
1.5			2.2949
2			1.6788
	3.5		4.0243
	4		4.4132
	4.5		4.7538
		0.4	3.5459
		0.6	3.5199
		0.8	3.4849

Table 2
Local skin associated friction quantity table of the various parameters.

A	We	Ha	β	$Re^{\frac{1}{2}}Cf_x$
1.0	3	0.2	3.5750	4.952713
1.5			2.2949	3.815798
2.0			1.6788	2.86247
	3.5		4.0243	5.641008
	4.0		4.4132	6.495281
		0.6	4.5199	5.039086
		0.8	3.4849	5.496822

are escalated for the higher values of *We*, *Ha,* and vice versa for *A* as shown in Table 2. Through Table 3, an uplift in the rate of heat balance is occurred, while taking higher values of *We*, ϵ, *Nb*, *Nt,* and σ, and decreasing in the rate of heat transfer is noticed with variation in the physical parameters, namely *A* and *Rd*. In the same table, a declination in the mass transfer rate is noticed during the variation in the *A*, λ_1, *Nt*, E_1 and δ. In this table, a higher rate of mass transfer during the variation in the *We*, ϵ, λ_1 and *Nb* is noted.

9. Comparison

In order to validate the entire results as determined during this particular investigation, a limiting case validation with the published work by (Wang, 2006 and Lit et al., 2016) is presented in Table 4. In particular, the comparison is provided in terms of skin friction with corresponding film thickness values. The entire validation shows an excellent correlation with the above-cited work while solving the problem numerically defined through equations (13–17).

Table 3
Heat and mass balance rates for various parameters values.

A	We	R_d	λ_1	ε	N_b	N_t	σ	E_1	δ	β	$Re^{-1/2}\ Nu_x$	$Re^{-1/2}\ Shu_x$
1	3	1	0.5	1	0.2	0.5	0.4	1	0.2	3.5750	0.5880215	1.086652
1.5											0.4805448	1.065109
2											0.4077060	1.085763
	3.5										0.5866644	1.191324
	4										0.5876978	1.034337
		1.5									0.4597303	1.086505
		2									0.3601310	1.086388
			−0.3								0.4920834	1.086939
			−0.5								0.4711717	1.086999
				1.2							0.6058031	1.086608
				1.4							0.6220108	1.086567
					0.3						0.5894588	1.120480
					0.4						0.5908903	1.137393
						0.6					0.5884394	1.066354
						0.7					0.5888863	1.046055
							0.5				0.5880386	1.093732
							0.6				0.5880552	1.100734
								1.2			0.5880072	1.080553
								1.4			0.5879957	1.075715
									0.3		0.5880159	1.083424
									0.4		0.5880096	1.079787

Table 4
Comparison of the previous results for different values of S.

S		0.4	0.6	0.8	1.0	1.2
(Wang, 2006)	β	5.1224900	3.1312500	2.1519900	1.5436200	1.1277800
	$f'(0)$	1.3077850	−1.195155	−1.245795	−1.277762	−1.279177
(Li et al., 2016)	β	4.981455	3.131924	2.152366	1.543592	1.127783
	$f'(0)$	−1.1340	−1.1950	−1.2460	−1.2780	−1.2790
Present outcomes	β	5.065799	3.136360	2.159388	1.599634	1.153103
	$f'(0)$	−1.133696	−1.195017	−1.245409	−1.271877	−1.274095

10. Conclusion

The entire new study was presented with new physical phenomenon namely, thin film flow over a moving surface. But, this new concept in the flow of time dependent Cross nanoliquid was addressed with some more physical impacts in the form of magnetic field, variable thermal conductivity, thermal radiation, heat generation/absorption and activation energy. However, for the higher values of Wessenberg number the velocity of the liquid was uplifted, while an opposite conduct was observed for Hartmann number. The film thickness was found in reducing conduct. The temperature was observed in enrichment behavior for higher values of Brownian motion and variable thermal conductivity parameters. The Brownian motion parameter, was increasing nanoparticle concentration and an opposite trend was observed for thermophoretic parameter. The concentration of the liquid was reducing function of activation energy parameter.

Declaration of competing interest

The authors declare that they have no known competing financial interests or personal relationships that could have appeared to influence the work reported in this paper.

References

Abbas, I.A., Palani, G., 2010. Effects of magnetohydrodynamic flow past a vertical plate with variable surface temperature. Appl. Math. Mech. 31, 329–338.

Acrivos, A., Shah, M.J., Petersen, E.E., 1960. Momentum and heat transfer in laminar boundary- layer flows of non-Newtonian fluids past external surface. J. A.I. Ch.E. 6 (2), 312–317.

Ahmad, L., Irfan, M., Javed, S., Khan, M.I., Khan, M.R., Niazi, U.M., El-Zahar, E.R., 2022. Influential study of novel microorganism and nanoparticles during heat and mass transport in Homann flow of visco-elastic materials. Int. Commun. Heat Mass Transf. 131, 105871.

Akbar, Y., Alotaibi, H., Iqbal, J., Nisar, K.S., Alharbi, K.A.M., 2022. Thermodynamic analysis for bioconvection peristaltic transport of nanofluid with gyrotactic motile microorganisms and Arrhenius activation energy. Case Stud. Thermal. Eng. 34, 102055.

Andersson, H.I., Aarseth, J.B., Braud, N., Dandapat, B.S., 1996. Flow of a power-law fluid film on unsteady stretching surface. J. Non- Newton Fluid Mech. 62 (1), 1–8.

Anjum, N., Khan, W.A., Hobiny, A., Azam, M., Waqas, M., Irfan, M., 2022. Numerical analysis for thermal performance of modified Eyring Powell nanofluid flow subject to activation energy and bioconvection dynamic. Case Studies Thermal Eng 39, 102427.

Ayub, A., Darvesh, A., Altamirano, G.C., Sabir, Z., 2021. Nanoscale energy transport of inclined magnetized 3D hybrid nanofluid with Lobatto IIIA scheme. Heat Transf. 50 (7), 6465–6490.

Ayub, A., Sabir, Z., Shah, S.Z.H., Mahmoud, S.R., Algarni, A., Sadat, R., Ali, M.R., 2022. Aspects of infinite shear rate viscosity and heat transport of magnetized Carreau nanofluid. The Eur. Phys. J. Plus. 137 (2), 247.

Ayub, A., Sabir, Z., Wahab, H.A., Balubaid, M., Mahmoud, S.R., Ali, M.R., Sadat, R., 2022. Analysis of the nanoscale heat transport and Lorentz force based on the time-dependent Cross nanofluid. Eng. Comput. 1–20. https://doi.org/10.1007/s00366-021-01579-1.

Aziz, R.C., Hashim, I., 2010. Liquid film on unsteady stretching sheet with general surface temperature and viscous dissipation. Chin. Phys. Lett. 27, (11) 110202.

Aziz, R.C., Hashim, I., Alomari, A.K., 2011. Thin film flow and heat transfer on an unsteady stretching sheet with internal heating. Meccanica 46, 349–357.

Bachok, N., Ishak, A., Pop, I., 2012. Unsteady boundary-layer flow and heat transfer of a nanofluid over a permeable stretching/shrinking sheet. Int. J. Heat Mass Transf. 55 (7–8), 2102–2109.

Bestman, A.R., 1990. Natural convection boundary layer with suction and mass transfer in a porous medium. Int. J. Eng. Res. 14, 389–396.

Bilal, M., Ahmed, A. E. S., El-Nabulsi, R. A., Ahammad, N. A., Alharbi, K. A. M., Elkotb, M. A., SA, Z. A., 2022. Numerical analysis of an unsteady, electroviscous, ternary hybrid nanofluid flow with chemical reaction and activation energy across parallel plates. Micromachines. 13(6), 874.

Bird, R.B., 1976. Useful non-Newtonian models. Annu. Rev. Fluid Mech. 8 (1), 13–34.

Bird, R.B., Curtiss, C.F., Armstrong, R.C., Hassager, O., 1987. Dynamics of polymeric liquids. John Wiley and Sons, New York.

Buongiorno, J., 2006. Convective transport in nanofluids. ASME. J. Heat Transf. 128, 240–250.

Chabani, I., Mebarek-Oudina, F., Vaidya, H., Ismail, A.I., 2022. Numerical analysis of magnetic hybrid Nano-fluid natural convective flow in an adjusted porous trapezoidal enclosure. J. Mag. Magnet. Mat. 564, 170142.
Choi, U.S., 1995. Enhancing thermal conductivity of fluids with nanoparticles. ASME. Int. Mech. Eng. Congress Expo. 66, 99–105.
Crane, L.J., 1970. Flow past a stretching plate. Zeitschrift Angew. Math. Phys. ZAMP 21, 645–647.
Cross, M.M., 1965. Rheology of non-Newtonian fluids: a new flow equation for pseudoplastic systems. J. Colloid Sci. 20 (5), 417–437.
Ghanmi, A., Abbas, I.A., 2019. An analytical study on the fractional transient heating within the skin tissue during the thermal therapy. J. Thermal Biol. 82, 229–233.
Haider, A., Ayub, A., Madassar, N., Ali, R.K., Sabir, Z., Shah, S.Z., Kazmi, S.H., 2021. Energy transference in time-dependent Cattaneo-Christov double diffusion of second-grade fluid with variable thermal conductivity. Heat Transf. 50 (8), 8224–8242.
Hassanien, I.A., Abdullah, A.A., Gorla, R.S.R., 1998. Flow and heat transfer in a power- law fluid over a non-isothermal stretching sheet. Math. Comput. Model. 28, 105–116.
Hayat, T., Khan, M.I., Tamoor, M., Waqas, M., Alsaedi, A., 2017. Numerical simulation of heat transfer in MHD stagnation point flow of Cross fluid model towards a stretched surface. Res. Phys. 7, 1824–1827.
Hobiny, A.D., Abbas, I.A., 2018. Theoretical analysis of thermal damages in skin tissue induced by intense moving heat source. Int. J. Heat Mass Transf. 124, 1011–1014.
Hobiny, A.D., Abbas, I.A., 2020. Fractional order thermo-elastic wave assessment in a two- dimension medium with voids. Geomech. Eng. 21 (1), 85–93.
Horrigue, S., Abbas, I.A., 2020. Fractional-order thermoelastic wave assessment in a two- dimensional fiber-reinforced anisotropic material. Mathematics 8 (9), 1609.
Hsiao, K.L., 2017. To promote radiation electrical MHD activation energy thermal extrusion manufacturing system efficiency by using Carreau-nanofluid with parameters control method. Energy 130, 486–499.
Jamil, S., Janjua, M.R.S.A., 2017. Synthetic study and merits of Fe 3O4 nanoparticles as mmerging material. J. Clust. Sci. 28, 2369–2400.
Jamil, S., Ahmad, H., Khan, S.R., Janjua, M.R.S.A., 2018. The first morphologically controlled synthesis of a nanocomposite of graphene oxide with cobalt tin oxide nanoparticles. RSC Adv. 8 (64), 36647–36661.
Jamil, S., Khan, S.R., Sultana, B., Hashmi, M., Haroon, M., Janjua, M.R.S.A., 2018. Synthesis of saucer shaped manganese oxide nanoparticles by co-precipitation method and the application as fuel additive. J. Clust. Sci. 29, 1099–1106.
Jamil, S., Zahra, G., Janjua, M.R.S.A., 2023. Morphologically controlled synthesis, characterization and applications of molybdenum oxide (MoO3) nanoparticles. J. Phys. Organic Chem. e4477.
Khan, W.A., Irfan, M., Khan, M., Alshomrani, A.S., Alzahrani, A.K., Alghamdi, M.S., 2017. Impact of chemical processes on magneto nanoparticle for the generalized Burgers fluid. J. Mol. Liq. 234, 201–208.
Khan, M., Manzur, M., Rahman, M., 2017. On axisymmetric flow and heat transfer of Cross fluid over a radially stretching sheet. Res. Phys. 7, 3767–3772.
Khan, W.A., Pop, I., 2010. Boundary-layer flow of a nanofluid past a stretching sheet. Int. J. Heat Mass Transf. 53 (11–12), 2477–2483.
Khan, M.I., Qayyum, S., Hayat, T., Waqas, M., Khan, M.I., Alsaedi, A., 2018. Entropy generation minimization and binary chemical reaction with Arrhenius activation energy in MHD radiative flow of nanomaterial. J. Mol. Liq. 259, 274–283.
Kumar, R., Gupta, V., Abbas, I.A., 2013. Plane deformation due to thermal source in fractional order thermoelastic media. J. Comput. Theoret. Nanosci. 10 (10), 2520–2525.
Lazaridis, F., Savara, A., Argyrakis, P., 2014. Reaction efficiency effects on binary Chemical reactions. J. Chem. Phys. 141, (10) 104103.
Li, J., Liu, L., Zheng, L., Bin-Mohsin, B., 2016. Unsteady MHD flow and radiation heat transfer of nano-fluid in a finite thin film with heat generation and thermophoresis. J. Taiwan Institute Chemi. Engi. 67, 226–234.
Lin, Y.H., Zheng, L.C., Li, B.T., Zhang, X.X., 2014. MHD thin film and heat transfer of power law fluids over an unsteady stretching sheet with variable thermal conductivity. Thermal Sci. 20 (6), 1791–1800.
Lin, Y.H., Zheng, L.C., Zhang, X.X., Mad, L.X., Chen, G., 2015. MHD pseudo-plastic nano-fluid unsteady flow and heat transfer in a finite thin film over stretching surface with internal heat generation. Int. J. Heat Mass Transf. 84, 903–911.
Manzur, M., Rahman, M., Khan, M., 2020. Computational study of Falkner Skan flow of chemically reactive Cross nano-fluid with heat generation or absorption. Phys. A: Statist. Mech. Appl. 554, 124267.
Mohamed, R.A., Abbas, I.A., Abo-Dahab, S.M., 2009. Finite element analysis of hydromagnetic flow and heat transfer of a heat generation fluid over a surface embedded in a non-Darcian porous medium in the presence of chemical reaction. Commun. Nonlin. Sci. Num. Simul. 14 (4), 1385–1395.
Mustafa, M., Khan, J.A., Hayat, T., Alsaedi, A., 2017. Buoyancy effects on the MHD nanofluid flow past a vertical surface with chemical reaction and activation energy. Int. J. Heat Mass Transf. 108, 1340–1346.
Naz, S., Bibi, G., Jamil, S., Rehman, S., Bibi, S., Ali, S., Janjua, M.R.S.A., 2022. Preparation of manganese-doped tin oxide nanoparticles for catalytic reduction of organic dyes. Chem. Phys. Lett. 802, 139768.
Palani, G., Abbas, I.A., 2009. Free convection MHD flow with thermal radiation from an impulsively-started vertical plate. Nonlinear Anal.: Model. Control 14 (1), 73–84.
Rehman, S., Alqahtani., H, S., Hadj Hassine, S.B., M. Eldin, S., 2023. Thermohydraulic and irreversibility assessment of Power-law fluid flow within wedge shape channel. Arabian J. Chem., 16(3), 104475.
Sakiadis, B.C., 1961. Boundary-layer behavior on continuous solid surfaces: I. Boundary-layer equations for two-dimensional and axisymmetric flow. AIChE J. 7 (1), 26–28.
Schowalter, W.R., 1960. The application of boundary-layer theory to power-law pseudoplastic fluids: Similar solutions. AIChE J. 6 (1), 24–28.
Shafique, Z., Mustafa, M., Mushtaq, A., 2016. Boundary layer flow of Maxwell fluid in rotating frame with binary chemical reaction and activation energy. Res. Phys. 6, 627–633.
Shah, S.L., Ayub, A., Dehraj, S., Wahab, H.A., Sagayam, K.M., Ali, M.R., Sabir, Z., 2022. Magnetic dipole aspect of binary chemical reactive Cross nanofluid and heat transport over composite cylindrical panels. Waves Random Complex Media 1–24. https://doi.org/10.1080/17455030.2021.2020373.
Shah, S.Z.H., Fathurrochman, I., Ayub, A., Altamirano, G.C., Rizwan, A., Nunez, R.A.S., Yeskindirova, M., 2022. Inclined magnetized and energy transportation aspect of infinite shear rate viscosity model of Carreau nanofluid with multiple features over wedge geometry. Heat Transf. 51 (2), 1622–1648.
Shao, Y., Ahmad, L., Javed, S., Ahmed, J., Elmasry, Y., Oreijah, M., Guedri, K., 2022. Heat and mass transfer analysis during Homann Visco-elastic slippery motion of nano-materials. Int. Commun. Heat Mass Transf. 139, 106425.
Ullah, I., Ali, F., Mohamad Isa, S, Murtaza, S., Jamshed, W., Mohamed, R. E., Amjad, A., Guedri, K., Khalifa, H. Abd El-W., Din, S.M. E., 2023. Electro-magnetic radiative flowing of Williamson-dusty nanofluid along elongating sheet: Nanotechnology application, Arabian J. Chem., 16(5), 104698.
Wang, C.Y., 1990. Liquid film on an unsteady stretching surface. Q. Appl. Math. 48 (4), 601–610.
Wang, C., 2006. Analytic solutions for a liquid film on an unsteady stretching surface. Heat Mass Transf. 42, 759–766.
Wang, F., Sajid, T., Ayub, A., Sabir, Z., Bhatti, S., Shah, N.A., Ali, M.R., 2022. Melting and entropy generation of infinite shear rate viscosity Carreau model over Riga plate with erratic thickness: a numerical Keller Box approach. Waves Random Complex Media 1–25. https://doi.org/10.1080/17455030.2022.2063991.
Wang, F., Ahmed, A., Khan, M.N., Ahammad, N.A., Alqahtani, A.M., Eldin, S.M., Abdelmohimen, M.A.H., 2023. Natural convection in nanofluid flow with chemotaxis process over a vertically inclined heated surface. Arab. J. Chem. 16, (4) 104599.
Xu, H., Pop, I., You, X.C., 2013. Flow and heat transfer in a nano-liquid film over an unsteady stretching surface. Int. J. Heat Mass Transf. 60, 646–652.